# Robustness Quantification of MIMO-PI Controller From the Perspective of $\gamma$-Dissipativity

Zimao Sheng[a], Shuxiang Yang[a], Hong'an Yang[a,*] and Rongkun Guo[a]

[a]School of Mechanical Engineering, Northwestern Polytechnical University, Xi'an, Shaanxi, 710072, China
[b] School of Artificial Intelligence, Tianjin University of Science and Technology, Tianjin, 300457, China

ARTICLE INFO

*Keywords*:
MIMO-PI controller
$\gamma$-dissipativity
parameter tuning
disturbed nonlinear MIMO system
eigenvalue problem (EVP)

ABSTRACT

The proportional-integral-derivative (PID) controller and its variants are widely used in control engineering, but they often rely on linearization around equilibrium points and empirical parameter tuning, making them ineffective for multi-input-multi-output (MIMO) systems with strong coupling, intense external disturbances, and high nonlinearity. Moreover, existing methods rarely explore the intrinsic stabilization mechanism of PID controllers for disturbed nonlinear systems from the perspective of modern robust control theories such as dissipativity and $\mathcal{L}_2$-gain. To address this gap, this study focuses on $\gamma$-dissipativity (partially equivalent to $\mathcal{L}_2$-gain) and investigates the optimal parameter tuning of MIMO-PI controllers for general disturbed nonlinear MIMO systems. First, by integrating dissipativity theory with the Hamilton-Jacobi-Isaacs (HJI) inequality, sufficient conditions for the MIMO-PI-controlled system to achieve $\gamma$-dissipativity are established, and the degree of $\gamma$-dissipativity in a local region containing the origin is quantified. Second, an optimal parameter tuning strategy is proposed, which reformulates the $\gamma$-dissipativity optimization problem into a class of standard eigenvalue problems (EVPs) and further converts it into linear matrix inequality (LMI) formulations for efficient online computation. Comprehensive simulation experiments validate the effectiveness and optimality of the proposed approach. This work provides a theoretical basis for the robust stabilization of general disturbed nonlinear MIMO systems and enriches the parameter tuning methods of PID controllers from the perspective of dissipativity.

## 1. INTRODUCTION

### 1.1. Motivation

For a long time, the classical proportional-integral-derivative (PID) controller has played an irreplaceable role in the field of control systems engineering[1]. Currently, mainstream variant methods of PID controllers tend to linearize and decouple complex nonlinear systems around their equilibrium points for approximation. Based on equilibrium point characteristics, parameter tuning strategies are designed using experimental methods such as Ziegler-Nichols rules[2], frequency-domain internal model control (IMC)[3], and the Indirect Design Approach (IDA)[4]. However, these methods struggle to stabilize multi-input-multi-output (MIMO) systems with strong coupling between state variables, intense external disturbances, and high nonlinearity. Moreover, most of these methods are empirical and fail to investigate the intrinsic mechanism by which PID controllers can stabilize disturbed nonlinear systems from the perspectives of passivity and the $\mathcal{L}_2$-gain of system disturbance energy in modern robust control theory[5, 6]. For disturbed nonlinear systems, robustly stable systems should typically exhibit dissipativity[7], meaning that the abstract "energy storage functions" of the system should be attenuated to a certain extent under the influence of disturbance noise. Systems with this property can often achieve a certain degree of Lyapunov stability and Input-to-State Stability (ISS)[8, 7] under specific conditions. We have further proven that such dissipative characteristics ensure asymptotic stability against bounded-energy disturbances in the $\mathcal{L}_2$ space. In this study, we start from a special type of $\gamma$-dissipativity, which is partially equivalent to the $\mathcal{L}_2$-gain of the system. The key questions then arise: For general disturbed nonlinear systems, what PID controller parameters should be designed to endow the entire system with dissipativity? Furthermore, how to optimize the controller parameters to maximize the system's dissipativity? In our previous work[9], we designed a MIMO-PI controller for general disturbed nonlinear systems and obtained the optimal parameter tuning strategy by optimizing the exponential rate at which control system errors converge to the global attractor near the origin and the size of the attractor. However, this method did not involve the optimization of system dissipativity near the origin or even along the entire state trajectory. This inspires us to propose a parameter design method for MIMO-PI controllers with optimal $\gamma$-dissipativity, targeting general disturbed nonlinear MIMO systems from the perspective of $\gamma$-dissipativity.

### 1.2. Related work

In contrast to classical PID controllers designed for linear single-input single-output (SISO) plants, significant research efforts have been dedicated in recent years to investigating the robust stabilization problem of PID controllers for nonlinear multi-input multi-output (MIMO) systems subject to disturbances. For instance, Zhong et al. [10] proposed an active disturbance rejection control (ADRC)-based tuning rule for MIMO non-affine uncertain systems with model uncertainty, to enable robust stabilization and decoupling

*Corresponding author
yhongan@nwpu.edu.cn (H. Yang)
ORCID(s): 0000-0001-6067-3379 (Z. Sheng); 0009-0004-0842-3750 (S. Yang); 0000-0001-5426-0041 (H. Yang); 0009-0001-6876-7334 (R. Guo)

control of the systems. Xiang et al. [11] incorporated adaptive single-parameter tuning to eliminate the requirement for manual trial-and-error tuning in the presence of nonlinearities and uncertainties. Wang et al. [12] further developed a deep reinforcement learning (DRL)-based adaptive PID tuning strategy for setpoint tracking in systems with time-varying uncertainty. However, these investigations primarily target nonlinear systems with specific structures, and most primarily address model uncertainty as opposed to externally imposed disturbances. For systems with external disturbances and nonlinearities, existing research [13, 14, 15] tends to directly linearize the nonlinear systems into linear time-invariant (LTI) models for controller parameter design. This approach aggregates nonlinear terms and external disturbances into a single component, treating them collectively as noise. Nevertheless, the controller parameters obtained via linearization around the equilibrium point often struggle to cope with plants exhibiting significant nonlinear characteristics.

Theoretically, it is fully achievable to accomplish local or even global robust stabilization of nonlinear disturbed MIMO systems through appropriate controller parameter tuning. For example, Zhao et al. [16, 17, 18] theoretically established sufficient conditions for guaranteeing effective error stabilization of PID controllers for general nonlinear uncertain MIMO systems. Jinke et al. [19] further proposed an explicit method to construct PID parameters by leveraging the upper bounds of derivatives of unknown nonlinear drift and diffusion terms in stochastic mechanical systems with white noise and linear inputs.

However, the core challenge lies not only in ensuring asymptotic stability or even exponential stabilization of the error dynamics for disturbed systems. Instead, we aim to design a suite of practically viable metrics that can quantify the robustness performance of MIMO-PI controllers when stabilizing the most general nonlinear disturbed systems. On this basis, we can optimize the system robustness by adjusting the controller parameters. It is worth noting that in our previous work [9], we have designed optimal robust controllers adopting two robustness metrics: the exponential convergence rate of the disturbed system error and the size of the ultimate invariant set of convergence.

Classical robust controller design methods typically aim to minimize the $H_\infty$ norm of the disturbed system to mitigate the impact of disturbances. For example, Gopmandal et al. [20] enhanced the hybrid search approach based on LTI static output feedback (SOF) from the perspective of $H_\infty$-synthesis for MIMO linear time-variant (LTV) systems with norm-bounded time-varying uncertain matrices. Nevertheless, no universally accepted metric exists for quantifying the $H_\infty$ norm of nonlinear disturbed systems, which has posed a bottleneck for the optimal parameter tuning of MIMO-PI controllers for such systems.

### 1.3. Contributions

Analogous to the $H_\infty$ norm for linear systems, concepts such as $\gamma$-dissipativity [21, 22] and $\mathcal{L}_2$-gain [23] in dissipativity theory enable the characterization of energy dissipation behaviors of disturbed nonlinear dynamical systems in an abstract framework, with more relevant results available in Ref. [7]. Building upon our prior work, we present the following contributions from the perspective of $\gamma$-dissipativity of disturbed nonlinear dynamical systems:

- For the most general nonlinear MIMO model with external disturbances, we establish sufficient conditions for the MIMO-PI-controlled system to attain $\gamma$-dissipativity through the integration of dissipativity theory and the Hamilton-Jacobi-Isaacs (HJI) inequality, and quantify the degree of $\gamma$-dissipativity in a local region containing the origin;
- From the perspective of optimizing the $\gamma$-dissipativity of the controlled system, we develop an optimal parameter tuning strategy for the MIMO-PI controller. This strategy reformulates the $\gamma$-dissipativity optimization problem of the disturbed nonlinear MIMO system as a class of standard eigenvalue problems (EVPs), which can be further converted into linear matrix inequality (LMI) formulations for efficient online computation. Comprehensive simulation experiments validate the effectiveness and optimality of the proposed approach.

Herein, we adopt the following general notations: $\|x\|$ denotes the 2-norm of vector $x$; $\lambda_{\max}[Re(A)]$ represents the maximum value of the real parts of the eigenvalues of matrix $A$; $\sup_{x\in\Omega} A(x)$ and $\inf_{x\in\Omega} A(x)$ denote the supremum and infimum of function $A(x)$ over the region $x \in \Omega$, respectively; $\frac{\partial f}{\partial x}$ denotes the Jacobian matrix of the vector function $f$ with respect to the independent variable $x$.

## 2. PRELIMINARIES

In this section, we introduce the concept of $\gamma$-dissipativity, which is a key component of modern robust control theory, and briefly describe its essential property. Building on this, we propose a MIMO-PI controller for more generalized multi-input multi-output (MIMO) nonlinear perturbed systems, which serve as the foundation for subsequent developments.

### 2.1. $\gamma$-dissipativity

In this section, we first introduce the concepts of a special class of $\gamma$-dissipativity and $\mathcal{L}_2$-gain, as presented in Definition 1 and 2. These concepts are natural extensions of the $H_\infty$ norm for linear perturbed systems in modern control theory. Furthermore, we establish the connection between them as shown in Lemma 1. In Lemma 2, we prove that nonlinear $\gamma$-dissipativity systems are asymptotically stable with respect to finite-energy disturbances under certain conditions. Finally, we present a sufficient condition for a nonlinear perturbed system to be $\gamma$-dissipativity, known as the HJI inequality (see Lemma 3).

**Definition 1.** *($\gamma$-dissipativity) For the nonlinear error system with disturbances $\dot{e} = f(e, \Omega)$, if there exists a smooth, continuously differentiable, and positive semi-definite storage function $V(e) \geq 0$ satisfying $V(0) = 0$, such that the inequality*

$$\dot{V}(e) \leq \frac{1}{2}\left(\gamma^2\|\Omega\|^2 - \|e\|^2\right) \tag{1}$$

*holds for all admissible disturbance inputs $\Omega$ (where $\gamma > 0$), then the system is referred to as $\gamma$-dissipativity.*

**Definition 2.** *($\mathcal{L}_2$-gain) For the nonlinear perturbed system $\dot{e}(t) = f(e(t), \Omega(t))$, $t \in [0, T]$, state $e(t) \in \mathbb{R}^n$, $e(t_0) = e_0$, disturbance $\Omega(t) \in \mathbb{R}^m$, if there exists $\gamma > 0$ such that*

$$\sqrt{\frac{\int_0^T ||e(\tau)||^2 d\tau}{\int_0^T ||\Omega(\tau)||^2 d\tau}} \leq \gamma \tag{2}$$

*then the system is said to exhibits the $\mathcal{L}_2$-gain property.*

**Lemma 1.** *For a given $\gamma > 0$, if the disturbed system is $\gamma$-dissipativity for zero-initial state $e(0) = 0$, then it possesses an $\mathcal{L}_2$-gain less than or equal to $\gamma$.*

*Proof.* See Appendix A for the proof. □

**Lemma 2.** *(Asymptotic stability of $\gamma$-dissipativity system) For the nonlinear system $\dot{e}(t) = f(e(t), \Omega(t))$, $t \in \mathbb{R}^+$, $e(t) \in \mathbb{R}^n$, $e(t_0) = e_0$, $\Omega(t) \in \mathbb{R}^m$, if the following conditions are satisfied: (1) there exists a smooth, continuously, and positive semi-definite storage function $V(e(t)) \geq 0$ satisfying $V(0) = 0$, such that the system is $\gamma$-dissipativity; (2) there exists $\bar{\lambda} > 0$ such that $V(e(t)) \leq \bar{\lambda}||e(t)||^2$; (3) $\int_0^\infty ||\Omega(\tau)||^2 d\tau = C_\Omega < \infty$. Then, $e(t) \to \{e : V(e) = 0\}$, as $t \to \infty$. Besides, if there exists $\alpha \in \mathcal{K}(.)$ such that $V(e(t)) \geq \alpha(||e(t)||)$,then $e(t) \to 0$ as $t \to \infty$.*

*Proof.* See Appendix B for the proof. □

It is evident that systems with the $\gamma$-dissipativity property exhibit strong robustness, which is reflected not only in ensuring a bounded $\mathcal{L}_2$-gain for the disturbed system but also in guaranteeing its asymptotic stability under finite-energy disturbances. Additionally, this robustness can be quantified by the $\gamma$. Next, a sufficient condition for determining whether the disturbed system is $\gamma$-dissipativity is provided.

**Lemma 3.** *(HJI-inequality) The necessary and sufficient condition for system $\dot{e} = f(e) + g(e)\omega$, $z = h(e)$, where the state $e \in \mathbb{R}^n$, $f(0) = 0$, the disturbance $\omega \in \mathbb{R}^m$, to be $\gamma$-dissipativity is that there exists a smooth and differentiable storage function $V(e)$ such that the following Hamilton-Jacobi-Issacs(HJI)-inequality*

$$\frac{\partial V}{\partial e} f(e) + \frac{1}{2\gamma^2}\frac{\partial V}{\partial e} g(e) g^T(e)\left[\frac{\partial V}{\partial e}\right]^T + \frac{1}{2} h^T(e) h(e) \leq 0 \tag{3}$$

*admits a semi-positive definite $V(e) \geq 0$ with $V(0) = 0$.*

*Proof.* See Ref. [7] for the proof. □

**Lemma 4.** *(Schur Complement Lemma) For a given symmetric matrix $S = \begin{bmatrix} S_{11} & S_{12} \\ S_{21} & S_{22} \end{bmatrix}$, where $S_{11} \in \mathbb{R}^{r\times r}$. The following three conditions are equivalent. (1) $S < 0$; (2) $S_{11} < 0, S_{22} - S_{12}^T S_{11}^{-1} S_{12} < 0$; (3) $S_{22} < 0, S_{11} - S_{12} S_{22}^{-1} S_{12}^T < 0$.*

*Proof.* See Ref. [24] for the proof. □

## 2.2. Eigenvalues of Hurwitz matrix

In the following Lemma 5, we present a method to determine the existence of a common characteristic matrix that satisfies the Lyapunov inequality for all countably many Hurwitz matrices. Notably, this lemma plays a crucial role in verifying the existence of the common matrix $P$ involved in Theorem 1.

**Lemma 5.** *For $A_i \in \mathbb{R}^{n\times n}$, $i = 1, 2, \ldots N$, $L_{A,i} = \sup_{1\leq j\leq N}\left\|A_j - A_i\right\|$, if*

$$Re\left[\lambda\left(A_i\right)\right] \leq -\varepsilon \tag{4}$$

*and*

$$\varepsilon > \min_{1\leq i\leq N}\left\{L_{A,i} M^2\left(A_i\right)\right\} \tag{5}$$

*where $\left\|e^{A_i^T t}\right\| \leq M\left(A_i\right) e^{-\varepsilon t}$, then there exists $P = P^T > 0$ such that $A_i P + P A_i^T + \varepsilon^* I \leq O$ for any $A_i, \varepsilon^* > 0$ holds.*

*Proof.* We can construct such a

$$P = \int_0^\infty e^{A_0^T t} Q e^{A_0 t} dt \tag{6}$$

where

$$A_0 = \text{argmin}_{i=1,2\ldots N}\left\{\left[\sup_j\left\|A_j - A_i^T\right\|\right] M^2\left(A_i\right)\right\} \tag{7}$$

It's obvious that $P = P^T > O$, let $F(t) = e^{A_0^T t} Q e^{A_0 t}$, $Q = Q^T > O$, its differential can be described as

$$\frac{dF(t)}{dt} = A_0^T e^{A_0^T t} Q e^{A_0 t} + e^{A_0^T t} Q e^{A_0 t} A_0 \tag{8}$$

Meanwhile, define $S_i(t) = A_i e^{A_0^T t} Q e^{A_0 t} + e^{A_0^T t} Q e^{A_0 t} A_i^T$, and

$$T_i(t) = S_i(t) - \frac{dF(t)}{dt} \tag{9}$$

$$= \underbrace{\left(A_i - A_0^T\right)}_{K_i} e^{A_0^T t} Q e^{A_0 t} + e^{A_0^T t} Q e^{A_0 t} \underbrace{\left(A_i^T - A_0\right)}_{K_i^T} \tag{10}$$

$$\begin{aligned} A_iP + PA_i^T &= \int_0^\infty A_iF(t) + F(t)A_i^T\,dt \\ &= \int_0^\infty S_i(t)dt = \int_0^\infty T_i(t) + \frac{dF(t)}{dt}dt \\ &= F(\infty) - F(0) + \int_0^\infty T_i(t)dt \\ &= -Q + \int_0^\infty T_i(t)dt \end{aligned} \tag{11}$$

Moreover, $\forall i$, $\left\|K_i\right\| = \left\|A_i - A_0^T\right\| \le \sup_i \left\|A_i - A_0^T\right\|$, and $\varepsilon > \sup_i \left\|A_i - A_0^T\right\| M^2(A_0) \ge \left\|K_i\right\| M^2(A_0)$, hence,

$$\begin{aligned} \int_0^\infty \left\|T_i(t)\right\| dt &\le \int_0^\infty 2\left\|K_i\right\| \left\|e^{A_0^T t} Q e^{A_0 t}\right\| dt \\ &\le 2\left\|K_i\right\| M^2\left(A_0\right)\|Q\| \int_0^\infty e^{-2\varepsilon t} dt \\ &= \frac{\left\|K_i\right\| M^2\left(A_0\right)\|Q\|}{\varepsilon} < \|Q\| \end{aligned} \tag{12}$$

Due to the fact that $\varepsilon > \left\|K_i\right\| M^2\left(A_0\right)$, thereby for any $\varepsilon^* > 0$, there exists $\alpha > 0$ such that

$$\frac{\left\|K_i\right\| M^2\left(A_0\right)}{\varepsilon} < 1 - \frac{\varepsilon^*}{\alpha} \tag{13}$$

For any $x \in \mathbb{R}^n$, let $Q = \alpha I$,

$$\begin{aligned} x^T\left(A_iP + PA_i^T\right)x &= x^T\left(-\alpha I + \int_0^\infty T_i(t)dt\right)x \\ &\le x^T\left(-\alpha + \int_0^\infty \left\|T_i(t)\right\| dt\right)x \\ &\le x^T\left(-\alpha + \left(1 - \frac{\varepsilon^*}{\alpha}\right)\|Q\|\,dt\right)x \\ &\le -\varepsilon^* x^T x \end{aligned} \tag{14}$$

Hence, $A_iP + PA_i^T + \varepsilon^* I \le O$ holds for any $A_i$ holds. □

**Remark 1.** *For Lemma 5, the inequality* $\left\|e^{A^T t}\right\| \le M(A)e^{-\varepsilon t}$ *holds, where* $\varepsilon = -\lambda_{\max}\left[Re(A)\right] > 0$, $M(A) = \sup_t \left\|e^{(A^T+\varepsilon I)t}\right\|$. *By performing the Jordan decomposition on* $A^T$, *we have* $A^T = \mathcal{P}\mathcal{J}\mathcal{P}^{-1}$, *where* $\mathcal{P}$ *is an invertible matrix and* $\mathcal{J}$ *is a Jordan matrix. Then* $M(A)$ *can be computed as follows:*

$$\begin{aligned} M(A) = \sup_{t>0}\left\|\mathcal{P}e^{(\mathcal{J}+\varepsilon I)t}\mathcal{P}^{-1}\right\| &\le \underbrace{\|\mathcal{P}\|\left\|\mathcal{P}^{-1}\right\| \sup_{t>0}\left\|e^{(\mathcal{J}+\varepsilon I)t}\right\|}_{\tilde{M}(A)} \\ s.t. \quad \mathcal{J} + \varepsilon I &\le O \end{aligned} \tag{15}$$

*We can adopt* $\tilde{M}(A)$ *as an estimation of* $M(A)$. *Particularly, if the Jordan canonical form* $\mathcal{J}$ *of* $A^T$ *is a purely diagonal matrix (i.e.,* $A^T$ *is diagonalizable), then we have* $\sup_{t>0}\left\|e^{(\mathcal{J}+\varepsilon I)t}\right\| = 1$. *In this case, the constant* $M(A)$ *in the inequality simplifies to the product of the norm of the similarity transformation matrix and its inverse:* $M(A) = \|\mathcal{P}\| \cdot \left\|\mathcal{P}^{-1}\right\|$.

### 2.3. MIMO-PI Controller

In this section, we analyze a general perturbed nonlinear system and propose a MIMO-PI controller[9]. Consider the following perturbed autonomous MIMO general nonlinear system within continuous and first-order differentiable $f \in \mathbb{R}^n$, and first-order differentiable disturbance $\omega(t) \in \mathbb{R}^l$,

$$\dot{e}(t) = f(e(t), u(t)) + \Gamma\omega(t),\ f(0,0) = 0 \tag{16}$$

where state $e(t) \in \mathbb{R}^n$, $e(t_0) = e_0$, control input $u(t) \in \mathbb{R}^m$, and $\Gamma \in \mathbb{R}^{n\times l}$. Further, we assume the adoption of a MIMO-PI controller that takes into account the coupling of multiple input channels. Explicitly,

$$u(t) = u(e(t)) = K_P e(t) + K_I \int_0^t e(t)dt \tag{17}$$

where $K_P \in \mathbb{R}^{m\times n}, K_I \in \mathbb{R}^{m\times n}$. Here, the control commands and its first-order derivative quantity are constrained as

$$u_{\min} \le u(t) \le u_{\max}, \dot{u}_{\min} \le \dot{u}(t) \le \dot{u}_{\max} \tag{18}$$

where $u_{\min}, u_{\max}, \dot{u}_{\min}, \dot{u}_{\max}, \in \mathbb{R}^m$. We expect to exponentially stablize the Eq.(16) within minimum $\gamma$-dissipativity to resist the sudden disturbances.

## 3. MAIN RESULTS

### 3.1. The $\gamma$-dissipativity of MIMO-PI Controller

As the core of this paper, Theorem 1 not only reveals the rationale behind the $\gamma$-dissipativity of general nonlinear perturbed systems under the MIMO-PI controller, but also specifically presents a sufficient condition for the error trajectory to possess $\gamma$-dissipativity over a certain time interval. Meanwhile, in Corollary 2, we further provide a sufficient condition for the existence of the characteristic matrix in Theorem 1, more precisely from the perspective of the eigenvalues of the Jacobian of the error trajectory. In particular, this result indicates that the entire trajectory is more likely to exhibit higher $\gamma$-dissipativity when the Jacobian matrix has negative eigenvalues that are further from the imaginary axis.

**Theorem 1.** *For the perturbed autonomous system Eq.(16), the MIMO-PI controller Eq.(17) is adopted as the input. If there exists* $P = P^T > O$ *and* $\varepsilon > 1$ *for any trajectory* $e = e(t)$, $t \ge t_0$ *such that*

$$PA_K(e) + A_K^T(e)P + \varepsilon I \le O \tag{19}$$

*Then the system exhibits the* $\gamma^*$*-dissipativity property, here:*

$$\gamma^* = \inf_\gamma \left\{\gamma : (1-\varepsilon)I + \frac{1}{\gamma^2}PGG^TP \le O, \forall e\right\} \tag{20}$$

*where* $K = \left[K_P, K_I\right]$, $A_K(e) = D_1(e) + D_2(e)K$,

$$D_1(e) = \begin{bmatrix} \frac{\partial f}{\partial e} & O \\ I & O \end{bmatrix}, D_2(e) = \begin{bmatrix} \frac{\partial f}{\partial u} \\ O \end{bmatrix}, G = \begin{bmatrix} \Gamma \\ O \end{bmatrix} \tag{21}$$

*Moreover, for finite-energy disturbance* $\omega$: $\int_0^\infty \|\omega(\tau)\|^2 \, d\tau < \infty$, *the error* $e(t), \dot{e}(t) \to 0$ *as* $t \to \infty$.

*Proof.* Substituting the differential form of the MIMO-PI controller $\dot{u}(t) = K_P\dot{e}(t) + K_I e(t)$ into the velocity form of perturbed autonomous system

$$\ddot{e}(t) = \frac{\partial f}{\partial e}\dot{e}(t) + \frac{\partial f}{\partial u}\dot{u}(t) + \Gamma\dot{\omega}(t) \tag{22}$$

to obtain the state-space model of $s(t) = \left[\dot{x}(t)^T, x(t)^T\right]^T$ as

$$\underbrace{\begin{bmatrix} \ddot{e}(t) \\ \dot{e}(t) \end{bmatrix}}_{\dot{s}(t)} = \underbrace{\begin{bmatrix} \frac{\partial f}{\partial e} + \frac{\partial f}{\partial u}K_P & \frac{\partial f}{\partial u}K_I \\ I & O \end{bmatrix}}_{A_K(e)} \underbrace{\begin{bmatrix} \dot{e}(t) \\ e(t) \end{bmatrix}}_{s(t)} + \underbrace{\begin{bmatrix} \Gamma \\ O \end{bmatrix}}_{G} \dot{\omega}(t) \tag{23}$$

here $A_K(e)$ can be decomposed as,

$$A_K(e) = \underbrace{\begin{bmatrix} \frac{\partial f}{\partial e} & O \\ I & O \end{bmatrix}}_{D_1(e)} + \underbrace{\begin{bmatrix} \frac{\partial f}{\partial u} \\ O \end{bmatrix}}_{D_2(e)} \underbrace{\begin{bmatrix} K_P & K_I \end{bmatrix}}_{K} \tag{24}$$

Due to the fact that, when $\varepsilon > 1$:

$$\lim_{\gamma\to\infty} \left\{ (1-\varepsilon)I + \frac{1}{\gamma^2} PGG^T P \right\} = (1-\varepsilon)I < O \tag{25}$$

Hence, there exists $\gamma^*$ as shown in Eq.(25) such that

$$(1-\varepsilon)I + \frac{1}{\gamma^{*2}} PGG^T P \le O \tag{26}$$

We construct the positive define Lyapunov function $V(s) = \frac{1}{2}s^T Ps$, and its derivative can be expressed as:

$$\frac{\partial V}{\partial s} = s^T P, \; V(0) = 0 \tag{27}$$

Hence,

$$\begin{aligned} &\frac{\partial V}{\partial s}A_K(e)s + \frac{1}{2\gamma^{*2}}\frac{\partial V}{\partial s}GG^T\left[\frac{\partial V}{\partial s}\right]^T + \frac{1}{2}s^T s \\ &= \frac{1}{2}s^T\left[PA_K(e) + A_K(e)^T P + \frac{1}{\gamma^{*2}}PGG^T P + I\right]s \\ &= \frac{1}{2}s^T\left[PA_K(e) + A_K^T(e)P + \varepsilon I\right]s \\ &+ \frac{1}{2}s^T\left[(1-\varepsilon)I + \frac{1}{\gamma^{*2}}PGG^T P\right]s \\ &\le \frac{1}{2}s^T\left[PA_K(e) + A_K^T(e)P + \varepsilon I\right]s \le 0 \end{aligned} \tag{28}$$

According to Lemma 3, HJI-inequality holds, the system exhibits $\gamma^*$-dissipativity. Moreover, according to the Lemma 2, the proof is completed. □

**Remark 2.** *In Theorem 1, to guarantee the existence of a common positive definite* $P$ *specified in Eq.(19) for all* $e = e(t) \in \Omega$ *with* $t \ge t_0$, *we start from Lemma 5 and derive a sufficient condition for the obtaining of* $K$ *from the eigenvalue perspective as follows:*

$$Re\left[\lambda\left(A_K(e)\right)\right] \le -\varepsilon, \quad \forall e \in \Omega \tag{29}$$

*where,*

$$\varepsilon > \inf_{e\in\Omega}\left\{\sup_{\tilde{e}\in\Omega}\left\|A_K(\tilde{e}) - A_K(e)\right\| M_K^2(e)\right\} \tag{30}$$

*and* $\left\|\exp\left(A_K(e)t\right)\right\| \le M_K(e)\exp(-\varepsilon t)$. *Furthermore, since* $e(t) \to 0$ *as* $t \to \infty$, *it is evident that* $0 \in \Omega$. *Thus, let*

$$\begin{aligned} S_K(\Omega) &= \sup_{\tilde{e}\in\Omega}\left\|A_K(\tilde{e}) - A_K(0)\right\| M_K^2(0) \\ &\ge \inf_{e\in\Omega}\left\{\sup_{\tilde{e}\in\Omega}\left\|A_K(\tilde{e}) - A_K(e)\right\| M_K^2(e)\right\} \end{aligned} \tag{31}$$

*we can determine the* $\gamma_K^*(\Omega)$*-dissipativity of the nonlinear perturbed system by examining the negativity of the index* $\mathcal{L}_K(\Omega)$*:*

$$\mathcal{L}_K(\Omega) = \sup_{e\in\Omega}\lambda_{\max}\left[Re\left(A_K(e)\right)\right] + S_K(\Omega) < 0 \tag{32}$$

Under the above constraint, the dissipativity $\gamma_K^*(\Omega)$ for parameter $K$ can be described as:

$$\gamma_K^*(\Omega) = \sup_{\varepsilon_K>1}\inf_{\gamma}\left\{\gamma : (1-\varepsilon_K)I + \frac{1}{\gamma^2}P_K(\varepsilon_K)GG^T P_K(\varepsilon_K) \le O\right\} \tag{33}$$

According to the Proof of Lemma 5 in Appendix 2.2, $P_K(\varepsilon_K)$ takes the following form:

$$P_K(\varepsilon_K) = \varepsilon_K\left(1 - \frac{S_K(\Omega)}{\mathcal{L}_K(\Omega)}\right)\int_0^\infty e^{A_K(0)^T t}e^{A_K(0)t}dt \tag{34}$$

Combining Eq.(33) and Eq.(34), we can further derive the specific form of $\gamma_K^*(\Omega)$ as follows:

$$\gamma_K^*(\Omega) = \sup_{\varepsilon_K>1}\inf_{\gamma}\left\{\gamma : \frac{1-\varepsilon_K}{\varepsilon_K^2\left(1 - \frac{S_K(\Omega)}{\mathcal{L}_K(\Omega)}\right)^2} + \frac{1}{\gamma^2}\tilde{P}_K GG^T\tilde{P}_K \le O\right\} \tag{35}$$

where $\tilde{P}_K = \int_0^\infty e^{A_K(0)^T t}e^{A_K(0)t}dt$, i.e., the solution of Lyapunov function $A_K(0)^T\tilde{P}_K + \tilde{P}_K A_K(0) + I = O$.

The above results demonstrate that the MIMO-PI controller with $K$ as the adjustable parameter exhibits the property of $\gamma_K^*(\Omega)$-dissipativity in region $\Omega$ (encompassing the neighborhood of the origin) when the constraint $\mathcal{L}_K(\Omega) < 0$

is satisfied. Under such a constraint, the dissipativity level of the system can be quantified by $\gamma_K^*(\Omega)$. Besides, the above conclusions establish a criterion for determining whether the MIMO-PI controller is $\gamma$-dissipativity over the given region $\Omega$. Furthermore, over this $\gamma$-dissipativity region, we quantify the degree of dissipativity.

### 3.2. Parameter Tuning within Optimal $\gamma$-dissipativity

In this section, provided that the MIMO-PI controller renders the nonlinear perturbed system $\gamma$-dissipativity, we investigate the optimization problem of the parameter $K^*$ from the viewpoint of disturbance energy. Specifically, we aim to design the controller such that the $\mathcal{L}_2$-gain over the region $\Omega$ is minimized as:

$$\begin{aligned} K^* &= \arg\min_K \gamma_K^*(\Omega) \\ s.t.\ \mathcal{L}_K(\Omega) &< 0,\ A_K(0)^T \tilde{P}_K + \tilde{P}_K A_K(0) + I = O \end{aligned} \tag{36}$$

The core difficulty in solving the aforementioned optimization problem lies in determining the $\mathcal{L}_2$-gain $\gamma_K^*(\Omega)$ over the fixed domain $\Omega$. Furthermore, we can transform the aforementioned $\gamma_K^*(\Omega)$ into a class of canonical Eigenvalue Value Problem (EVP). Specifically, we aim to select an appropriate gain $K$ such that there exists a scalar $\varepsilon_K > 1$, so as to attain a minimized $\gamma$. This optimization problem can be rewrited as follows:

$$\min_K \gamma$$
$$s.t. \begin{cases} \left(1 - \frac{S_K(\Omega)}{\mathcal{L}_K(\Omega)}\right)^2 \tilde{P}_K G G^T \tilde{P}_K - \frac{(\varepsilon_K - 1)\gamma^2}{\varepsilon_K^2} I \le O \\ \mathcal{L}_K(\Omega) < 0 \end{cases} \tag{37}$$

Given that

$$\max_{\varepsilon_K > 1} \frac{(\varepsilon_K - 1)}{\varepsilon_K^2} = \frac{1}{4} \tag{38}$$

we further transform the aforementioned problem into the following Linear Matrix Inequality (LMI) form by virtue of the Schur Complement Lemma:

$$\begin{aligned} \gamma_K^*(\Omega) = \min_{K, \mathcal{L}_K(\Omega)<0} \gamma > 0 \\ s.t. \begin{bmatrix} O & 2\left(1 - \frac{S_K(\Omega)}{\mathcal{L}_K(\Omega)}\right) \tilde{P}_K G \\ 2\left(1 - \frac{S_K(\Omega)}{\mathcal{L}_K(\Omega)}\right) G^T \tilde{P}_K & O \end{bmatrix} \le \gamma I \end{aligned} \tag{39}$$

where $\tilde{P}_K$ satisfys that

$$K^T D_2(0)^T \tilde{P}_K + \tilde{P}_K D_2(0) K + D_1(0)^T \tilde{P}_K + \tilde{P}_K D_1(0) + I = O \tag{40}$$

We aim to realize optimal $\gamma$-dissipativity-based parameter tuning over the specified domain $\Omega$. This objective is attainable if there exists a parameter $K$ within $\Omega$ satisfying $\mathcal{L}_K(\Omega) < 0$. Once this condition is met, one can conduct an exhaustive search over all feasible parameters $K$ within the domain to retrieve the optimal parameter $K^* = \arg\max_K \gamma_K^*(\Omega)$ of MIMO-PI controller.

## 4. SIMULATION

In this section, we will verify the $\gamma$-dissipativity theory of the designed MIMO-PI controller through a specific control example of a perturbed nonlinear MIMO model. Furthermore, based on this theory, we will carry out the optimal design of controller parameters to verify the rationality of our optimal parameter tuning strategy.

### 4.1. Experimental configuration

For simplicity, we adopt the perturbed nonlinear controlled model from our prior work [9] as the benchmark. This model is a simplified kinematic model for designing robust path-following guidance laws of fixed-wing UAVs [25] in the ground coordinate system along the $\gamma$ and $\chi$ directions, expressed as follows:

$$\begin{aligned} \dot{\chi}(t) &= \frac{g \tan\phi(t)}{V} + d_\chi \\ \dot{\gamma}(t) &= \frac{g[n_z(t)\cos\phi(t) - \cos\gamma(t)]}{V} + d_\gamma \end{aligned} \tag{41}$$

Herein, the flight states of the kinematic model, $x(t) = \left[\gamma(t), \chi(t)\right]^T$, represent the flight path angle and course angle of the UAV at time $t$, respectively. The control input is defined as $u(t) = [\phi(t), n_z(t)]^T$, a vector comprising the roll angle $\phi(t)$ and the normal overload $n_z(t)$ along the z-axis direction. The term $d = [d_\chi, d_\gamma]^T$ denotes the disturbance imposed on $\dot{\chi}(t)$ and $\dot{\gamma}(t)$, induced by factors such as wind fields and model simplification. Specifically, the perturbation $d$ takes the form of sinusoidal noise signals: $d_\chi = L_{d_\chi}\sin(\omega_\chi t)$ and $d_\gamma = L_{d_\gamma}\cos(\omega_\gamma t)$. The aircraft velocity $V$ is assumed to be constant, and $g$ denotes the gravitational acceleration with a value of $9.81\mathrm{m/s}^2$. We define the reference tracking signals as $x_c = \left[\chi_c, \gamma_c\right]^T$, with the tracking error $e(t) = \left[e_\chi(t), e_\gamma(t)\right]^T$ given by $e(t) = x_c - x(t) = \left[\chi_c - \chi(t), \gamma_c - \gamma(t)\right]^T$. Under this error definition, the aforementioned perturbed system can be transformed into:

$$\underbrace{\begin{bmatrix} \dot{e}_\chi(t) \\ \dot{e}_\gamma(t) \end{bmatrix}}_{\dot{e}(t)} = \underbrace{\begin{bmatrix} -\frac{g\tan\phi(t)}{V} \\ -\frac{g(n_z(t)\cos\phi(t) - \cos(\gamma_c - e_\gamma(t)))}{V} \end{bmatrix}}_{f_e(e(t),u(t))} + \underbrace{\begin{bmatrix} -d_\chi \\ -d_\gamma \end{bmatrix}}_{d_e} \tag{42}$$

The Jacobians of $f_e(e,u)$ with respect to $e$ and $u$ are derived as follows:

$$\begin{aligned} \frac{\partial f_e(e,u)}{\partial e} &= \begin{bmatrix} 0 & 0 \\ 0 & \frac{g}{V}\sin(\gamma_c - e_\gamma) \end{bmatrix} \\ \frac{\partial f_e(e,u)}{\partial u} &= \begin{bmatrix} -\frac{g}{V}\sec^2\phi & 0 \\ \frac{gn_z}{V}\sin\phi & -\frac{g}{V}\cos\phi \end{bmatrix} \end{aligned} \tag{43}$$

The relevant model parameters are listed in Table 1.

**Table 1**
Hyperparameter declarations

| Declaration | Param | Value | Unit | Declaration | Param | Value | Unit |
|---|---|---|---|---|---|---|---|
| Simulation timespan | $T$ | [0,20] | s | Lipschitz constant of $d_\chi$ | $L_{d_\chi}$ | 0.1 | – |
| Acceleration of gravity | $g$ | 9.81 | m/s$^2$ | Lipschitz constant of $d_\gamma$ | $L_{d_\gamma}$ | 0.1 | – |
| Initial climb angle | $\gamma(0)$ | $\pi/4$ | rad | Disturbance frequency of $d_\chi$ | $\omega_\chi$ | 0.15 | rad/s |
| Initial azimuth angle | $\chi(0)$ | $\pi/3$ | rad | Disturbance frequency of $d_\gamma$ | $\omega_\gamma$ | 0.15 | rad/s |
| Initial roll angle | $\phi(0)$ | $\pi/3$ | rad | The range of $\phi$ | $[\phi_{\min},\phi_{\max}]$ | [$-\pi/4,\pi/4$] | rad |
| Initial overload | $n_z(0)$ | 1 | – | The range of $\dot{\phi}$ | $[\dot{\phi}_{\min},\dot{\phi}_{\max}]$ | [$-\pi/6,\pi/6$] | rad/s |
| Reference climb angle | $\gamma_c$ | $\pi/12$ | rad | The range of $n_z$ | $[n_{z,\min},n_{z,\max}]$ | [-2.1,2.1] | – |
| Reference azimuth angle | $\chi_c$ | 0 | rad | The range of $\dot{n}_z$ | $[\dot{n}_{z,\min},\dot{n}_{z,\max}]$ | [-1,1] | $/s$ |
| Reference roll angle | $\phi_c$ | 0 | rad | Consolidated velocity | $V$ | 25 | m/s |
| Reference overload | $n_{zc}$ | 0 | – | | | | |

## 4.2. Verification of $\gamma$-dissipativity domain for the MIMO-PI Controller

To stabilize the aforementioned perturbed system, we design a MIMO-PI controller as shown in Eq.(17). The optimal controller parameters $K = [K_P^*, K_I^*]$, derived in Ref. [9], are given as follows:

$$K_P^* = \begin{bmatrix} 1.6968 & 0.5906 \\ -0.5906 & 1.9556 \end{bmatrix}, K_I^* = \begin{bmatrix} 3.4869 & 0.1784 \\ -0.1784 & 3.4869 \end{bmatrix} \tag{44}$$

First, unlike $\mathcal{L}_K(\Omega)$ defined on region $\Omega$ containing the origin, we redefine the dissipativity index $\mathcal{L}_K(e)$ at an arbitrary point $e$ as:

$$\mathcal{L}_K(e) = \lambda_{\max}\left[\mathrm{Re}(A_K(e))\right] + \left\|A_K(e) - A_K(0)\right\| M_K^2(0) \tag{45}$$

It is evident that $\sup_{e\in\Omega}\mathcal{L}_K(e) \le \mathcal{L}_K(\Omega)$, i.e., $\mathcal{L}_K(e)$ at any point in region $\Omega$ serves as a lower bound of $\mathcal{L}_K(\Omega)$ and directly impacts the specific value of $\mathcal{L}_K(\Omega)$. Thus, we can quantify the point-wise dissipativity degree via $\mathcal{L}_K(e)$.

To this end, we select discretized grid points from $-\pi/3$ to $\pi/3$ with a step size of 0.05 along the $e_\chi$-axis and from $-\pi/6$ to $\pi/6$ with a step size of 0.01 along the $e_\gamma$-axis. $\mathcal{L}_K(e)$ values at each point in this rectangular grid region are calculated to evaluate the point-wise dissipativity index, with results shown in Figure 1. Notably, in the heatmap, $\mathcal{L}_K(e)$ exhibits uniformity along the horizontal direction of the $e_\chi$-axis, indicating that the error $e_\chi$ has no effect on system dissipativity. By contrast, $\mathcal{L}_K(e)$ is high at both ends and low in the middle along the horizontal direction of the $e_\gamma$-axis, and its distribution is symmetric about the line $e_\gamma = 0$, which implies that a larger absolute error $|e_\gamma|$ degrades system dissipativity and thus undermines robust stabilization. At the boundary where $\mathcal{L}_K(e) = 0$ (termed the zero line), $\mathcal{L}_K(e) > 0$ in regions outside this boundary, making it difficult to determine whether such regions possess $\gamma$-dissipativity.

Leveraging the heatmap characteristics, we use the width $W_K$ between the two zero lines along the $e_\gamma$-axis (referred to as the dissipativity domain) to characterize the measure of the dissipative region. In fact, a larger $W_K$ indicates wider regions where the MIMO-PI controller can achieve

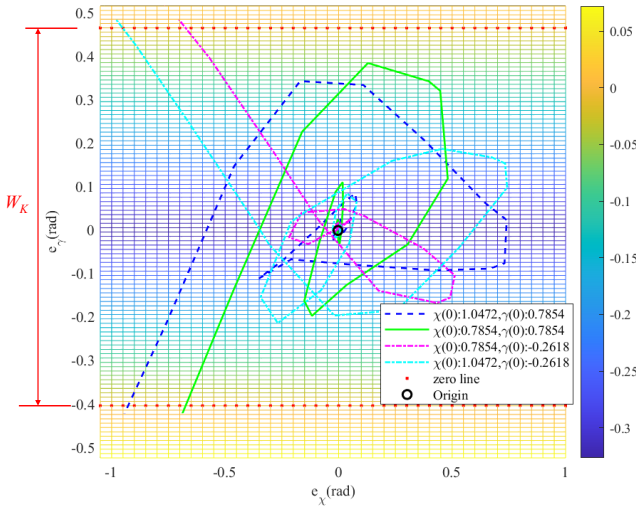


**Figure 1:** Two-dimensional phase portraits of error trajectories under different initial conditions $\chi(0)$ and $\gamma(0)$, which illustrate the error origin, $\mathcal{L}_{K^*}(e)$ at every point $e$, and the corresponding boundary of $\mathcal{L}_{K^*}(\Omega) = 0$ (zero line).

error $\gamma$-dissipativity under parameter $K$, enabling robust stabilization; conversely, a smaller $W_K$ corresponds to narrower dissipative regions, which is unfavorable for robust stabilization. Further, as shown in Figure 1, we design four groups of initial error conditions $e(0) = \left[\chi(0), \gamma(0)\right]^T$. It can be observed that regardless of the initial error, as long as the error trajectory remains within the $\gamma$-dissipativity domain, $e(t)$ will eventually converge to the vicinity of the origin. Moreover, in regions with weak $\gamma$-dissipativity (i.e., smaller $\left\|\mathcal{L}_K(e)\right\|$), state trajectories are relatively smooth, implying large fluctuations in the error convergence process; in regions with strong $\gamma$-dissipativity (i.e., larger $\left\|\mathcal{L}_K(e)\right\|$), trajectories are tortuous, which means the error convergence process is confined tightly near the origin and thus achieves stable convergence, corresponding to enhanced dissipativity and robustness.

The above conclusions demonstrate the rationality of using indices $\mathcal{L}_K(e)$ and $\mathcal{L}_K(\Omega)$ to quantify the $\gamma$-dissipativity degree of the nonlinear perturbed system under the MIMO-PI controller.

**Table 2**
The different rectangular region $\Omega$.

| Region | Range of $e_\chi$ | Range of $e_\gamma$ | Color |
|---|---|---|---|
| $\Omega_1$ | $[-0.7, 0.7]$ | $[-0.3, 0.3]$ | Magenta |
| $\Omega_2$ | $[-0.5, 0.5]$ | $[-0.22, 0.22]$ | Blue |
| $\Omega_3$ | $[-0.25, 0.25]$ | $[-0.15, 0.15]$ | Green |
| $\Omega_4$ | $[-0.1, 0.1]$ | $[-0.06, 0.06]$ | Red |

### 4.3. Verification of $\gamma$-dissipativity index $\gamma_K(\Omega)$

Currently, the widely adopted metric for evaluating the error stabilization performance of the controller is the average Integral Time Absolute Error (ITAE). It is defined as the time integral of the absolute tracking error over a specified time interval from $t = 0$ to $T$:

$$\text{ITAE} = \frac{1}{T}\int_0^T \|e(t)\|\, dt \tag{46}$$

We intend to use this metric to demonstrate the robustness quantification capability of the proposed index $\gamma_K(\Omega)$. To validate the rationality of our indictor $\gamma_K(\Omega)$, we derive new controller coefficients $K$ by introducing incremental perturbations $\Delta K$ to the baseline optimal coefficients $K^*$.

$$K = K^* + \Delta K = K^* - \varepsilon \left[I_p, I_i\right] \tag{47}$$

For simplicity, $\Delta K$ can be described in the form $\Delta K = -\varepsilon \left[I_p, I_i\right]$, where $I_p$ and $I_i$ both are identity matrixes, and $\epsilon \in \mathbb{R}^1$ is served as a regulation variable to determine $\Delta K$. We then compare the corresponding response curves and their associated ITAE across multiple $\varepsilon$, as shown in Table 3.

To achieve an objective, gradient-based visualization of the index $\gamma_K(\Omega)$ across different regions $\Omega$, we define four regions $\Omega_1, \Omega_2, \Omega_3, \Omega_4$ enclosed by rectangular boundaries for each parameter $K$, with their boundary lines and colors detailed in Table 2. Specifically, we calculate the index $\gamma_K(\Omega_i)$ for these four boundary regions, as presented in Table 3; their exact ranges are also visualized in Figure 2. Notably, both the zero line width $W_K$ and the index $\gamma_K(\Omega_i)$ for each region vary with different controller parameters $K$. A general trend is observed that $\gamma_K(\Omega_i)$ decreases for regions $\Omega_i$ closer to the origin. Since $\gamma_K(\Omega_i)$ theoretically represents the $\mathcal{L}_2$-gain of the error, regions with darker blue in the heatmaps exhibit smaller $\mathcal{L}_2$-gain, indicating stronger robustness against error disturbance energy. However, the parameter $K$ selected by minimizing $\gamma_K(\Omega_i)$ is not necessarily optimal, as a smaller $\gamma_K(\Omega_i)$ may lead to a narrower $W_K$ and thus reduce the scope of $\gamma$-dissipativity. For instance, compared with subfigure (b), subfigure (a) shows a smaller global $\gamma$-dissipativity index but a correspondingly narrower $W_K$.

Figure 4 provides a more intuitive illustration of the time-domain profiles of the absolute values of the error $e(t)$ and its derivative $\dot{e}(t)$ for different parameters $K$ corresponding to distinct $W_K$ and $\gamma_K(\Omega_i)$. In both subfigures, a smaller $\gamma_K(\Omega_i)$ tends to be associated with weaker oscillations and a smoother error stabilization process. For example, the blue curve, corresponding to the minimum $\gamma_K(\Omega_i)$, shows the flattest profile, whereas the brown-red dashed curve, with the maximum $\gamma_K(\Omega_i)$, exhibits the most severe fluctuations. From an energy perspective, minimizing $\gamma_K(\Omega_i)$ essentially maximizes the attenuation of disturbance energy, thereby reducing oscillation induced by perturbations and enhancing the system's dissipative performance. To further quantify the impact of $W_K$ on error convergence, Figure 4 also presents the relationships between $W_K$ and the ITAE as well as standard deviation indices of $e(t)$ and $\dot{e}(t)$ for different $K$. A strong negative correlation is clearly observed between $W_K$ and these two indices, implying that a wider $\gamma$-dissipativity domain generally leads to a more stable error stabilization process. Moreover, the standard deviation analysis reveals that $W_K$ has an exponential impact on the stability of the system's convergence process.

Furthermore, we compare the index $R_K$ proposed in our previous work[9]—describing the exponential convergence rate of errors under the MIMO-PI controller near the origin—with the indices $\gamma_K(\Omega_i)$ and $W_K$, as shown in Figure 5. In subfigure (a), a strong negative correlation between $R_K$ and $\gamma_K(\Omega_i)$ is evident for the origin-adjacent regions $\Omega_3$ and $\Omega_4$, which can be interpreted as stronger $\gamma$-dissipativity near the origin corresponding to a faster exponential convergence rate. However, for the regions $\Omega_1$ and $\Omega_2$ farther from the origin, enhanced dissipativity does not necessarily yield a faster convergence rate, which is mainly attributed to the larger region scope and sustained energy perturbations that may increase system uncertainty. Subfigure (b) further demonstrates the distinctiveness between the proposed index $W_K$ and $R_K$. If we aim to select parameters with both a high exponential convergence rate (larger $R_K$) and a wide $\gamma$-dissipativity domain (larger $W_K$), the peak point in the subfigure undoubtedly corresponds to the optimal parameter $K^*$, as it balances the trade-off between convergence rate and $\gamma$-dissipativity domain. This finding can serve as a key principle for subsequent parameter tuning.

## 5. CONCLUSION

This research primarily accomplishes the following key work:

- To quantify the correlation between the $\mathcal{L}_2$-gain of general perturbed nonlinear systems and controller parameters, we establish a sufficient criterion for $\gamma$-dissipativity of origin-containing regions;
- Building on this, we propose a dedicated index for quantifying regional $\gamma$-dissipativity, enabling the design of optimal controller parameters that maximize $\gamma$-dissipativity (i.e., minimize $\mathcal{L}_2$-gain);
- Experimental results validate the index's rationality and reveal consistency with our prior exponential convergence rate metric (near the origin), while exhibiting superior quantification capability across a wider operating range.

**Table 3**
The different $\epsilon$ and corresponding $R_K$, $W_K$, $\gamma_K(\Omega_1)$, $\gamma_K(\Omega_2)$, $\gamma_K(\Omega_3)$, $\gamma_K(\Omega_4)$.

| $K$ | $\epsilon$ | $R_K$ | $W_K$ | $\gamma_K(\Omega_1)$ | $\gamma_K(\Omega_2)$ | $\gamma_K(\Omega_3)$ | $\gamma_K(\Omega_4)$ | $K$ | $\epsilon$ | $R_K$ | $W_K$ | $\gamma_K(\Omega_1)$ | $\gamma_K(\Omega_2)$ | $\gamma_K(\Omega_3)$ | $\gamma_K(\Omega_4)$ |
|---|---|---|---|---|---|---|---|---|---|---|---|---|---|---|---|
| $K_1$ | -4 | 0.7742 | 0.8 | 11.16 | 5.97 | 4.23 | 3.06 | $K_4$ | 0.5 | 0.3626 | 0.87 | 15.98 | 9.31 | 6.82 | 5.07 |
| $K_2$ | -2 | 0.6754 | 0.96 | 8.46 | 5.72 | 4.42 | 3.41 | $K_5$ | 0.8 | 0.2849 | 0.69 | 75.92 | 16.92 | 10.05 | 6.68 |
| $K_3$ | -1 | 0.5913 | 0.98 | 9.65 | 6.52 | 5.03 | 3.89 | $K_6$ | 1 | 0.2192 | 0.54 | 30.80 | 61.61 | 17.03 | 9.04 |

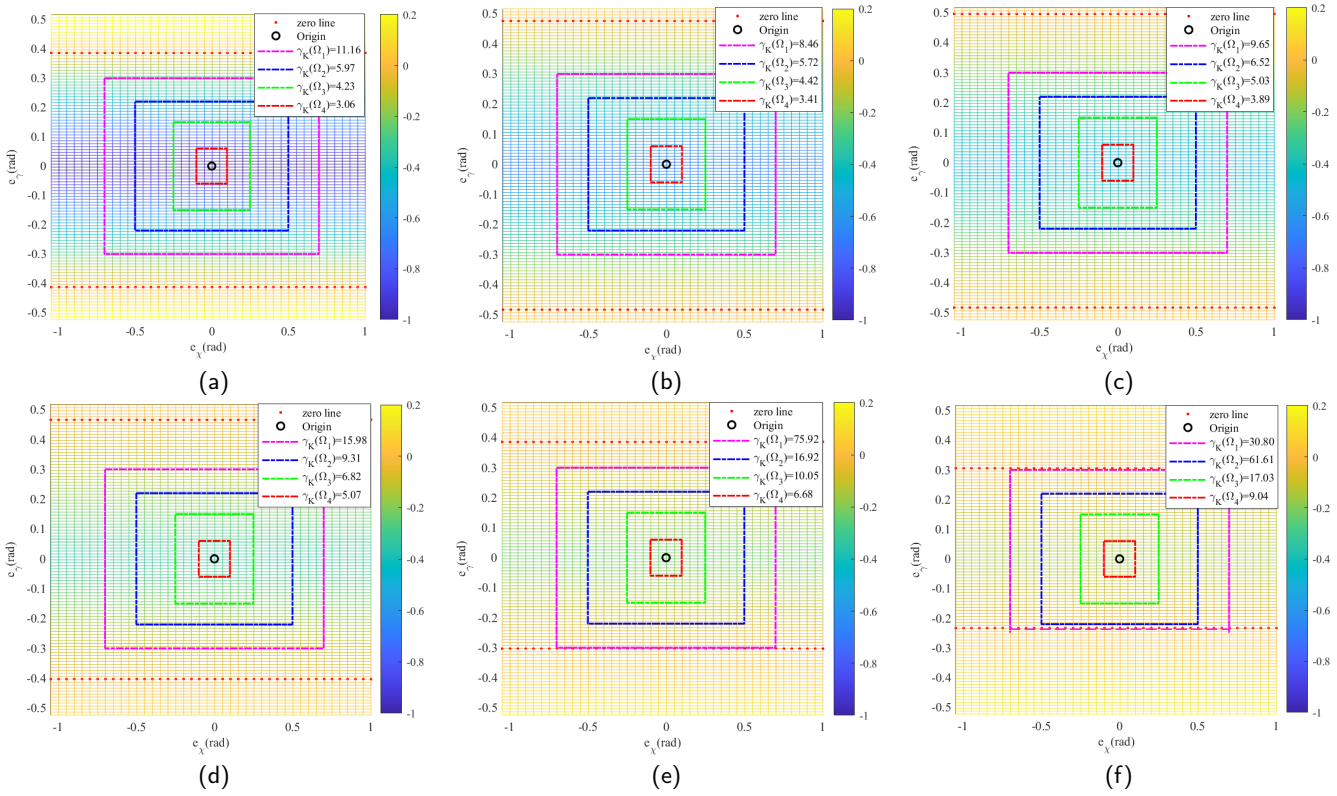


**Figure 2:** Dissipativity indices $\gamma_K(\Omega_i)$ over regions $\Omega_i, i = 1, 2, 3, 4$ for different controller parameters $K$. (a): For the $K_1$; (b): For the $K_2$; (c): For the $K_3$; (d): For the $K_4$; (e): For the $K_5$; (f): For the $K_6$.

Notably, practical deployment requires acquiring the controlled model's Jacobian matrix for optimal parameter tuning, future research will focus on Jacobian estimation under model-free scenarios to enhance engineering feasibility.

## ACKNOWLEDGEMENT

This work was supported by National Natural Science Foundation of China (Grant No. 51775435). The preprint can be accessed at https://arxiv.org/abs/2601.06568.

## References

[1] Tariq Samad. A survey on industry impact and challenges thereof [technical activities]. *IEEE Control Systems Magazine*, 37(1):17–18, 2017.

[2] Zhuo-Yun Nie, Zhaoyang Li, Qing-Guo Wang, Zhiqiang Gao, and Jiliang Luo. A unifying ziegler-nichols tuning method based on active disturbance rejection. *INTERNATIONAL JOURNAL OF ROBUST AND NONLINEAR CONTROL*, 32(18, SI):9525–9541, DEC 2022.

[3] Ramon Vilanova and Antonio Visioli. *PID control in the third millennium*, volume 75. Springer, 2012.

[4] Bharat Verma and Prabin Kumar Padhy. Robust fine tuning of optimal pid controller with guaranteed robustness. *IEEE Transactions on Industrial Electronics*, 67(6):4911–4920, 2019.

[5] Christopher I Byrnes, Alberto Isidori, Jan C Willems, et al. Passivity, feedback equivalence, and the global stabilization of minimum phase nonlinear systems. *IEEE Transactions on automatic control*, 36(11):1228–1240, 1991.

[6] Arjan van der Schaft. $l_2$-gain analysis of nonlinear systems and nonlinear state feedback $h_\infty$ control. *IEEE transactions on automatic control*, 37(6):770–784, 1992.

[7] David J. Hill and Tao Liu. Dissipativity, stability, and connections: Progress in complexity. *IEEE Control Systems Magazine*, 42(2):88–106, 2022.

[8] Eduardo D. Sontag and Yuan Wang. On characterizations of the input-to-state stability property. *Systems and Control Letters*, 24(5):351–359, 1995.

[9] Zimao Sheng, Hong'an Yang, Jiakang Wang, and Tong Zhang. Robust convergency indicator using mimo-pi controller in the presence of disturbances. *Journal of the Franklin Institute*, 362(17):108152, 2025.

[10] Sheng Zhong, Yi Huang, and Lei Guo. An adrc-based pid tuning rule. *INTERNATIONAL JOURNAL OF ROBUST AND NONLINEAR CONTROL*, 32(18, SI):9542–9555, DEC 2022.

[11] Kaili Xiang, Yongduan Song, and Petros Ioannou. Nonlinear adaptive pid control for nonlinear systems. *IEEE Transactions on Automatic Control*, pages 1–8, 2025.

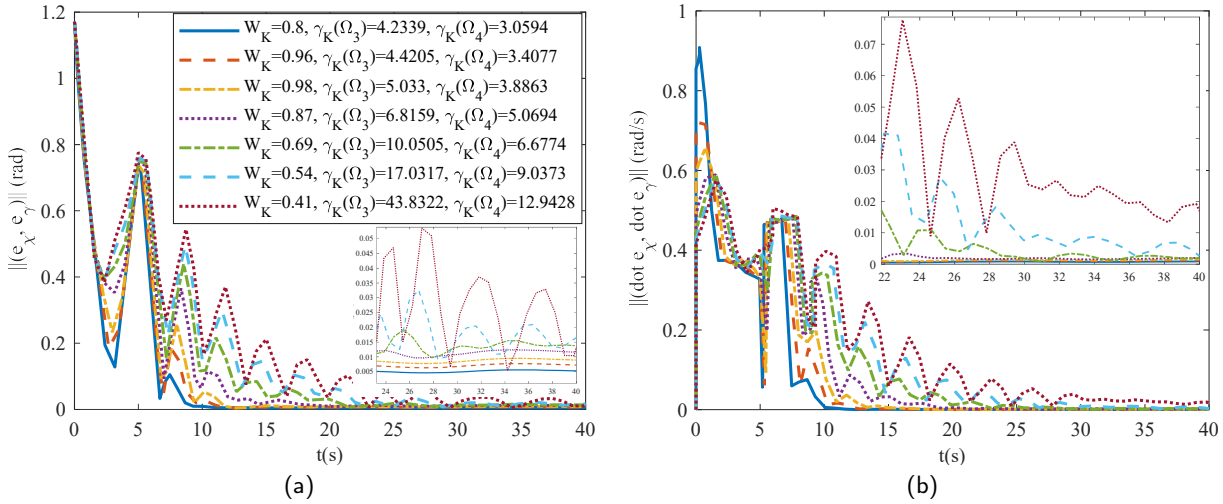


**Figure 3:** Time curves of the amplitudes of the error $e(t)$ and its derivative $\dot{e}(t)$ at the six different regions in Figure 2. (a): Time curves of the amplitudes of the error $e(t)$; (b): Time curves of the amplitudes of the error $\dot{e}(t)$.


[12] Hao Wang and Luis A. Ricardez-Sandoval. A deep reinforcement learning-based pid tuning strategy for nonlinear mimo systems with time-varying uncertainty. *IFAC PAPERSONLINE*, 58(14):887–892, 2024. 12th IFAC Symposium on Advanced Control of Chemical Processes (ADCHEM), Toronto, CANADA, JUL 14-17, 2024.

[13] Xinyi Yu, Peixuan Ding, Linlin Ou, and Weidong Zhang. General stabilization approach of the low-order controller for both siso systems and mimo systems with multiple time delays. *AUTOMATICA*, 166, AUG 2024.

[14] Luca Cavanini, Riccardo Felicetti, Francesco Ferracuti, and Andrea Monteriu. Error governor for active fault tolerance in pid control of mimo systems. *INTERNATIONAL JOURNAL OF SYSTEMS SCIENCE*, 56(7):1457–1473, MAY 19 2025.

[15] Sumit Kumar Pandey. A novel optimum decoupling and control of mimo systems based on linear matrix inequality and kharitonov theorem. *ENGINEERING LETTERS*, 33(5):1671–1683, MAY 2025.

[16] Cheng Zhao and Lei Guo. Towards a theoretical foundation of pid control for uncertain nonlinear systems. *Automatica*, 142:110360, 2022.

[17] Cheng Zhao and Lei Guo. Control of nonlinear uncertain systems by extended pid. *IEEE Transactions on Automatic Control*, 66(8):3840–3847, 2020.

[18] Cheng Zhao and Lei Guo. Pid controller design for second order nonlinear uncertain systems. *Science China Information Sciences*, 60:1–13, 2017.

[19] Jinke Zhang and Lei Guo. Pid control for high dimensional nonlinear uncertain stochastic systems. In *2019 Chinese Control Conference (CCC)*, pages 1501–1505. IEEE, 2019.

[20] Falguni Gopmandal and Arun Ghosh. A hybrid search based script capital $h_\infty$ synthesis of static output feedback controllers for uncertain systems with application to multivariable pid control. *INTERNATIONAL JOURNAL OF ROBUST AND NONLINEAR CONTROL*, 31(12):6069–6090, AUG 2021.

[21] Peter Moylan. Dissipative systems and stability. *Lecture Notes in collaboration with D. Hill, University of Newcastle, www. pmoylan. org*, 2014.

[22] Bernard Brogliato, Rogelio Lozano, Bernhard Maschke, Olav Egeland, et al. Dissipative systems analysis and control. *Theory and applications*, 2:2–5, 2007.

[23] Arjan Van der Schaft. *L2-gain and passivity techniques in nonlinear control*. Springer, 2000.

[24] Zhang Fuzhen. The schur complement and its applications. *Series: Numerical Methods and Algorithms*, 4, 2005.

[25] Ahmed S Rezk, Horacio M Calderón, Herbert Werner, Benjamin Herrmann, and Frank Thielecke. Predictive path following control for fixed wing uavs using the qlmpc framework in the presence of wind disturbances. In *AIAA SCITECH 2024 Forum*, page 1594, 2024.

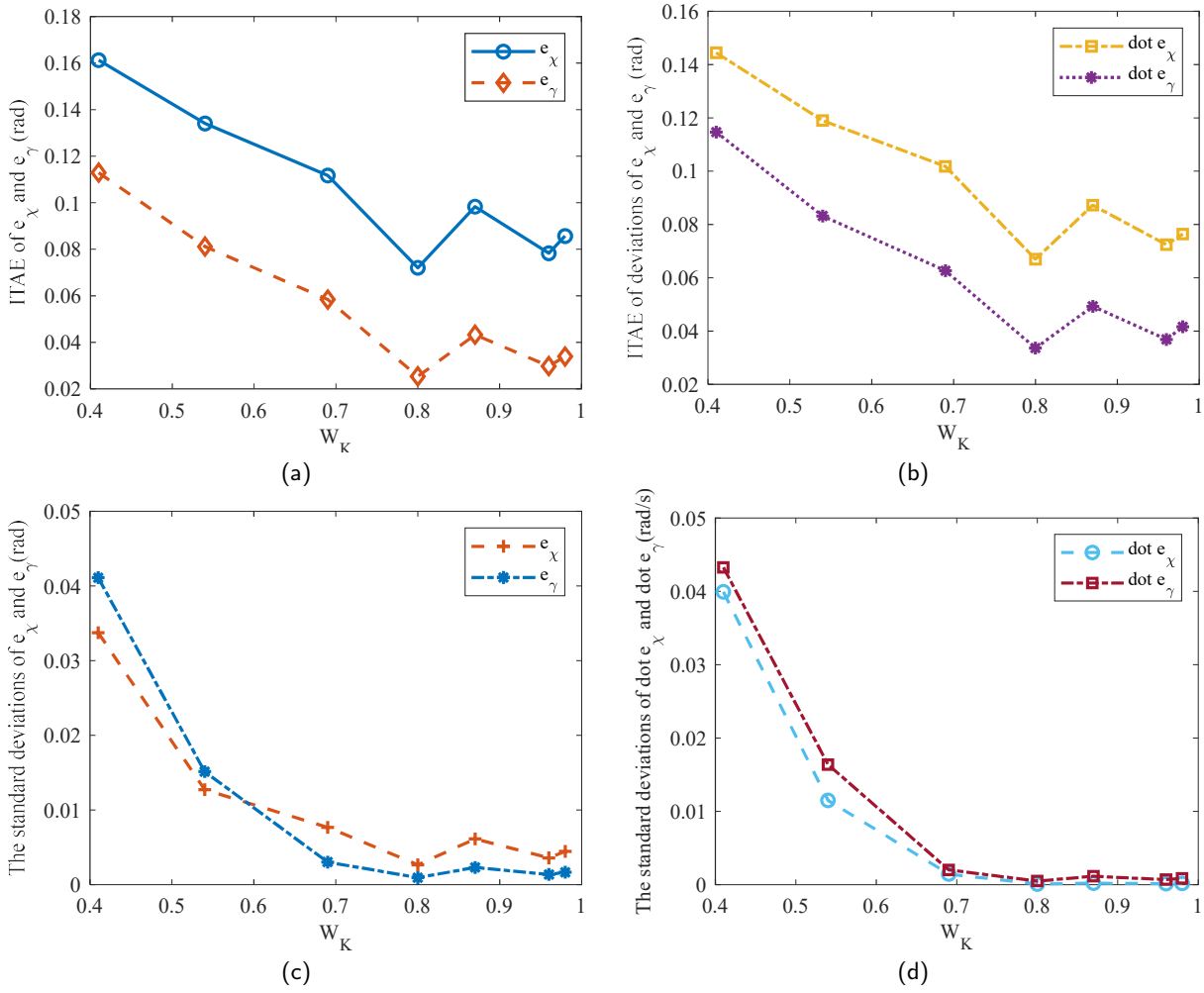


**Figure 4:** Relationships between indictor $W_K$ (different $K$) and ITAE/Standard deviation of $e_\chi, e_\gamma, \dot{e}_\chi, \dot{e}_\gamma$. (a): Relationships between $W_K$ and ITAE of $e_\chi$ and $e_\gamma$; (b): Relationships between $W_K$ and ITAE of $\dot{e}_\chi$ and $\dot{e}_\gamma$; (c): Relationships between $W_K$ and standard deviation of $e_\chi$ and $e_\gamma$; (d): Relationships between $W_K$ and standard deviation of $\dot{e}_\chi$ and $\dot{e}_\gamma$;

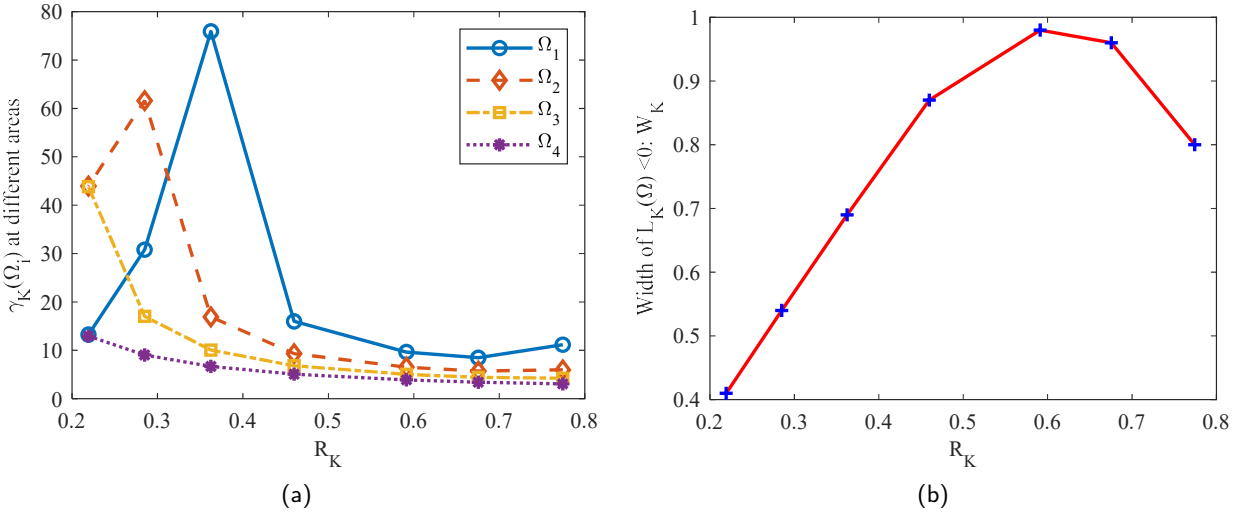


**Figure 5:** Curves of the relationships between the robustness index $R_K$ and $\gamma_K(\Omega_i)$ as well as $W_K$ respectively. (a): Relationship between $R_K$ and $\gamma_K(\Omega_i)$, $i = 1, 2, 3, 4$; (b): Relationship between $R_K$ and $W_K$.

## A. Proof of Lemma 1

*Proof.* At time $T$, if the system is $\gamma$-dissipativity, then its corresponding positive semi-definite storage function $V(e)$ for zero-initial state $e(0) = 0$ satisfies:

$$0 \leq V(e(T)) = V(e(T)) - V(0) \tag{48}$$

$$\leq \int_0^T \dot{V}(e(\tau))d\tau \tag{49}$$

$$\leq \int_0^T \frac{1}{2}\left(\gamma^2\|\Omega(\tau)\|^2 - \|e(\tau)\|^2\right)d\tau \tag{50}$$

Hence, there exists

$$\sqrt{\frac{\int_0^T ||e(\tau)||^2 d\tau}{\int_0^T ||\Omega(\tau)||^2 d\tau}} \leq \gamma \tag{51}$$

The proof is completed. □

## B. Proof of Lemma 2

*Proof.* From the $\gamma$-dissipativity property of positive semi-definite $V(e(t))$, there exists

$$\dot{V}(e(t)) \leq \frac{1}{2}\left(\gamma^2||\Omega(t)||^2 - ||e(t)||^2\right) \tag{52}$$

and

$$||e(t)||^2 \geq \frac{1}{\bar{\lambda}}V(e(t)) \tag{53}$$

such that, $\forall t \geq t_0$,

$$w(t) = \dot{V}(e(t)) + \frac{1}{2\bar{\lambda}}V(e(t)) - \frac{1}{2}\gamma^2||\Omega(t)||^2 \leq 0 \tag{54}$$

Hence, solving Eq.(54) yields:

$$\begin{aligned} V(e(t)) &= V(e_0)e^{-\frac{t-t_0}{2\bar{\lambda}}} \\ &+ \int_{t_0}^t e^{-\frac{t-\tau}{2\bar{\lambda}}}\left[w(\tau) + \frac{1}{2}\gamma^2||\Omega(\tau)||^2\right]d\tau \\ &\leq V(e_0)e^{-\frac{t-t_0}{2\bar{\lambda}}} + \frac{\gamma^2}{2}\int_{t_0}^t e^{-\frac{t-\tau}{2\bar{\lambda}}}||\Omega(\tau)||^2 d\tau \\ &= V(e_0)e^{-\frac{t-t_0}{2\bar{\lambda}}} + \frac{\gamma^2}{2}\left(\int_{t_0}^{\frac{t}{2}} + \int_{\frac{t}{2}}^t\right)e^{-\frac{t-\tau}{2\bar{\lambda}}}||\Omega(\tau)||^2 d\tau \end{aligned} \tag{55}$$

There exist $\tau^* \in [t_0, \frac{t}{2}]$ such that

$$\begin{aligned} 0 &\leq \int_{t_0}^{\frac{t}{2}} e^{-\frac{t-\tau}{2\bar{\lambda}}}||\Omega(\tau)||^2 d\tau = e^{-\frac{t-\tau^*}{2\bar{\lambda}}}\int_{t_0}^{\frac{t}{2}}||\Omega(\tau)||^2 d\tau \\ &\leq C_\Omega e^{-\frac{t-\tau^*}{2\bar{\lambda}}} \leq C_\Omega e^{-\frac{t}{4\bar{\lambda}}} \end{aligned} \tag{56}$$

Thus, $\lim_{t\to\infty}\int_{t_0}^{\frac{t}{2}} e^{-\frac{t-\tau}{2\bar{\lambda}}}||\Omega(\tau)||^2 d\tau = 0$.

In this case, it also holds for $t^* \in [\frac{t}{2}, t]$ simultaneously that

$$\begin{aligned} \int_{\frac{t}{2}}^t e^{-\frac{t-\tau}{2\bar{\lambda}}}||\Omega(\tau)||^2 d\tau &= ||\Omega(t^*)||^2\int_{\frac{t}{2}}^t e^{-\frac{t-\tau}{2\bar{\lambda}}}d\tau \\ &\leq 2\bar{\lambda}||\Omega(t^*)||^2\left(1 - e^{-\frac{t}{4\bar{\lambda}}}\right) \end{aligned} \tag{57}$$

Due to the fact that $\int_0^\infty ||\Omega(\tau)||^2 d\tau = C_\Omega < \infty$, there exists $||\Omega(t^*)||^2 \to 0$, as $t^* \to \infty$. Thus,

$$\lim_{t\to\infty}\int_{\frac{t}{2}}^t e^{-\frac{t-\tau}{2\bar{\lambda}}}||\Omega(\tau)||^2 d\tau \to 0 \tag{58}$$

Thus,

$$\lim_{t\to\infty} V(e(t)) = 0 \tag{59}$$

Hence, in the case of $||e(t)|| \leq \alpha^{-1}(V(e(t)))$, there exists

$$\lim_{t\to\infty}||e(t)|| = 0 \tag{60}$$

The proof is completed. □